Springer

Journal of
Mechanical
Science and
Technology

Journal of Mechanical Science and Technology 22 (2008) 293~299

www.springerlink.com/content/1738-494x

Cutting force model considering tool edge geometry for micro end milling process

Ik Soo Kang[1,*], Jeong Suk Kim[2] and Yong Wie Seo[3]

[1]*Engineering Research Center for Net Shape and Die Manufacturing, Pusan National University, Jangjeon-dong, Geumjeong-gu, Busan 609-735, Korea*

[2]*School of Mechanical Engineering, Pusan Nationl University, Jangjeon-dong, Geumjeong-gu, Busan 609-735, Korea*

[3]*School of Mechanical and Automotive Engineering, Inje University, Obang-dong, Gimhae, Gyeongnam 621-749, Korea*

(Manuscript Received November 11, 2006; Revised November 21, 2007; Accepted November 21, 2007)

Abstract

The analysis of the cutting force in micro end milling plays an important role in characterizing the cutting process, as the tool wear and surface texture depend on the cutting forces. Because the depth of cut is larger than the tool edge radius in conventional cutting, the effect of the tool edge radius can be ignored. However, in micro cutting, this radius has an influence on the cutting mechanism. In this study, an analytical cutting force model for micro end milling is proposed for predicting the cutting forces. The cutting force model, which considers the edge radius of the micro end mill, is simulated. The validity is investigated through the newly developed tool dynamometer for the micro end milling process. The predicted cutting forces were consistent with the experimental results.

Keywords: Cutting force; Micro end milling; Tool edge radius; Micro cutting

1. Introduction

As demands for micro parts are on the increase in recent industries such as aerospace, biomedical, electronics, environment, information technology and display, the need for manufacturing such parts is also increasing. Major methods of manufacturing micro parts are based on non-traditional machining, such as lithography, etching, lasers, ultrasonic, ion-beam and electrical discharge [1, 2]. However, the material removal rate of these methods is relatively slow, and workpiece materials and applicable shapes are limited. Therefore, mechanical machining is required for the manufacturing of micro parts with complex shapes.

The end milling process can be applied to the manufacturing of a variety of shapes from macro to micro scale levels. Recently, the application of micro end milling process has been increasing for the parts that cannot be manufactured by MEMS technology. The diameter of the micro end mill that is used in micro end milling is very small; it takes more time and costs may be wasted because tools are fractured easily. It is also difficult to monitor the tool conditions. Accordingly, the cutting force analysis plays an important role in the establishment of machining plans, the selection of cutting conditions, and the investigation of cutting process characteristics, such as tool wear and surface texture in micro end milling.

In the milling process, the cutting force analysis was first introduced by Martellotti [3], and Tlusty and MacNeill [4] proposed the investigation of analytic cutting forces in the conventional end milling process. Tlusty and MacNeil's model expressed cutting force as a function of undeformed chip thickness. In addition, a similar model was proposed by Kline and DeVor [5]. Study on three-dimensional cutting force model have been conducted by Yucesan et al. [6]. An analytic cutting force model of micro end milling was

*Corresponding author. Tel.: +82 51 510 3079, Fax.: +82 51 518 7207
E-mail address: iskang@pusan.ac.kr
DOI 10.1007/s12206-007-1110-x

first introduced by Bao and Tansel [7]. This model is based on Tlusty and MacNeil's model and takes into account the differences of the trajectory of the tool tip between micro end milling and conventional end milling. Unlike macro cutting, the effect of the tool edge radius cannot be ignored in micro cutting because the depth of cut reaches the scale order of the tool edge radius. Accordingly, this study presents an analytic model that considers the tool edge radius and performs a verification of the cutting force characteristics in high-speed micro end milling.

2. Cutting force model

2.1 Micro cutting mechanism

When the depth of cut is larger than the tool edge radius, the effect of the tool edge radius can be ignored. However, in micro cutting, the ploughing at the tool edge and the sliding on the flank face are the dominant parameters for the cutting force regarding the major cutting mechanism [8-10].

When the effect of the tool edge radius is taken into consideration in micro cutting, the principal cutting force F_C and thrust force F_T can be expressed as the following Eqs. (1) and (2):

$$F_C = F_{CC} + F_{SC} \tag{1}$$

$$F_T = F_{CT} + F_{ST} \tag{2}$$

where F_{CC} and F_{CT} are the force components by shearing, and F_{SC} and F_{ST} are the force components by sliding.

As shown in Fig. 1, F_{CC} and F_{CT} represent the force components acting on a shear plane. Accordingly, F_{CC} and F_{CT} can be expressed as the following Eqs. (3) and (4):

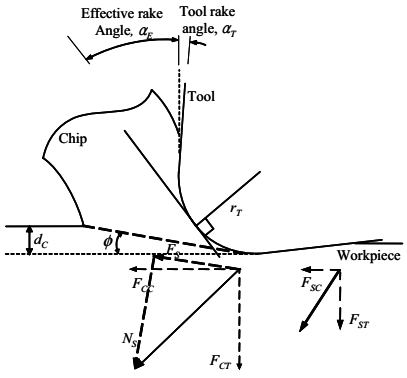

Fig. 1. Cutting force vectors and effective rake angle at tool edge.

$$F_{CC} = F_S \cos\phi + N_S \sin\phi \tag{3}$$

$$F_{CT} = -F_S \sin\phi + N_S \cos\phi \tag{4}$$

where F_S is the shear force in the shear plane, N_S is the normal force in the shear plane and ϕ is the shear angle.

It is supposed that the forces acting on the shear plane are uniformly distributed and the shear stress complies with the yield criterion of von Mises. Then the shear force F_S and the normal force N_S can be expressed as the following Eqs. (5) and (6):

$$F_S = \bar{\sigma} b d_C / \sqrt{3} \sin\phi \tag{5}$$

$$N_S = \bar{\sigma} b d_C / \sin\phi \tag{6}$$

$$\bar{\sigma} = K_M \bar{\varepsilon}^n$$

where $\bar{\sigma}$ is the flow stress, b is the width of cut, d_C is the depth of cut, K_M is the compensated strength coefficient, $\bar{\varepsilon}$ is the strain, and n is the work-hardening exponent.

F_{SC} and F_{ST} are the force components by the sliding. The sliding is caused by the elastic recovery of the workpiece on the flank face, which acts additionally when considering the tool edge radius. The force elements caused by the sliding are divided into cutting and thrust directions. It is supposed that they are dependent on the yield strength. F_{SC} and F_{ST} can be expressed as the yield strength and contact area as the following Eqs. (7) and (8):

$$F_{SC} = Y_M l_C b / \sqrt{3} \tag{7}$$

$$F_{ST} = Y_M l_C b \tag{8}$$

where Y_M is the compensated yield strength, and l_C is the contact length of the tool and workpiece on the flank face.

The existing models depend on the specific cutting force obtained through experiments, but this model is dependent on the flow stress and the yield strength related to the material property. In micro cutting, the yield strength has a considerably great value due to the size effect. Also, the flow stress is increased due to the high strain rate. Accordingly, the experiments were conducted to compensate K_M and Y_M for the flow stress and yield strength [11].

The contact length l_C was obtained from the relief angle of the tool and the spring back due to the elastic recovery occurring on the flank face by Arcona and Dow's model [12]. The contact length l_C can be ob-

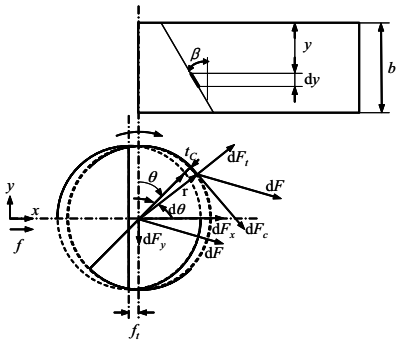

Fig. 2. Force direction and variation of undeformed chip thickness in end milling process.

tained with the following Eq. (9):

$$l_C = S/\sin\theta_F \qquad (9)$$
$$S = k_1 r_T H_V / E$$

where S is the springback of the workpiece, θ_F is the relief angle of the tool, k_1 is the constant, r_T is the tool edge radius, H_V is the Vicker's hardness and E is the elastic modulus.

When the depth of cut is less than the tool edge radius in micro cutting, the cutting force behavior, as indicated in Fig. 1, is similar to the grinding process in which the rake angle has a negative value. The contributions to total cutting energy are the chip formation and the sliding and ploughing caused by the effective rake angle [13, 14]. The depth of cut d_C in two-dimensional cutting can be expressed as the undeformed chip thickness t_C in end milling in Fig. 2. As the depth of cut is varied, the shear angle is also varied. The shear angle is determined according to the undeformed chip thickness. Merchant's model was used for the prediction of the shear angle. The effective rake angle is adopted as the rake angle when the depth of cut is below the tool edge radius and a tool rake angle is adopted as the rake angle when the depth of cut is above the tool edge radius. The effective rake angle α_E can be obtained geometrically as shown in Eq. (10):

$$\alpha_E = \cos^{-1}(1-\frac{d_C}{r_T}) - \frac{\pi}{2} \qquad (10)$$

2.2 Cutting force for micro end milling

In this study, Tlusty and MacNeil's model [4] was used for the prediction of undeformed chip thickness in the end milling process. The undeformed chip thickness t_C can be expressed as:

$$t_C = f_t \sin\theta = d_C \qquad (11)$$

where f_t is the feed per tooth and θ is the tool rotation angle.

When the undeformed chip thickness t_C is substituted for the depth of cut d_C, F_C and F_T can be represented as follows:

$$\mathrm{d}F_C = \left(\frac{\bar{\sigma} f_t\, r}{\sqrt{3}\tan\phi}\sin\theta + \bar{\sigma} f_t\, r\sin\theta + \frac{\mathrm{Y_M} l_C r}{\sqrt{3}}\right)\mathrm{dy} \qquad (12)$$

$$\mathrm{d}F_T = \left(-\frac{\bar{\sigma} f_t\, r}{\sqrt{3}}\sin\theta + \frac{\bar{\sigma} f_t\, r}{\tan\phi}\sin\theta + \mathrm{Y_M} l_C r\right)\mathrm{dy} \qquad (13)$$

$$\mathrm{d}y = \frac{r}{\tan\beta}\mathrm{d}\theta \qquad (14)$$

where r is the tool radius, dy is the cutting element depending on the helix angle, β is the helix angle.

In the principal cutting force Eq. (12) and thrust force Eq. (13), the first and second terms represent the element of shear force, and the third term indicates the sliding force.

The resultant cutting force can be divided into the two components of feed(x) and normal(y) directions shown in Fig. 2. The feed direction cutting force F_x and the normal direction cutting force F_y can be expressed as follows:

$$\mathrm{d}F_x = -\mathrm{d}F_C\cos\theta - \mathrm{d}F_T\sin\theta \qquad (15)$$
$$\mathrm{d}F_y = \mathrm{d}F_C\sin\theta - \mathrm{d}F_T\cos\theta \qquad (16)$$

When Eqs. (15) and (16) are integrated from the tool start angle θ_s to the tool end angle θ_e, the final feed and normal direction cutting forces can be obtained as follows:

$$F_x = [\, C_1(\sin 2\theta_e - \sin 2\theta_s) + C_2(\cos 2\theta_e - \cos 2\theta_s) - C_3(\sin\theta_e - \sin\theta_s) + C_4(\cos\theta_e - \cos\theta_s) - 2C_1(\theta_e - \theta_s)] \qquad (17)$$

$$F_y = [\, -C_2(\sin 2\theta_e - \sin 2\theta_s) + C_1(\cos 2\theta_e - \cos 2\theta_s) - C_4(\sin\theta_e - \sin\theta_s) - C_3(\cos\theta_e - \cos\theta_s) + 2C_2(\theta_e - \theta_s)] \qquad (18)$$

where

$$C_1 = \frac{\bar{\sigma} f_t\, r}{4\tan\phi\tan\beta} - \frac{\bar{\sigma} f_t\, r}{4\sqrt{3}\tan\beta},$$

$$C_2 = \frac{\bar{\sigma} f_t r}{4\sqrt{3}\tan\phi\tan\beta} + \frac{\bar{\sigma} f_t r}{4\tan\beta},$$

$$C_3 = \frac{Y_M l_C r}{\sqrt{3}\tan\beta}, \quad C_4 = \sqrt{3}\, C_3$$

3. Micro cutting experiment

When the spindle revolution is low in the micro end milling process with a small tool, the quality of the machined surface and tool life can deteriorate due to the low cutting speed. To increase cutting speed, a machine tool has to rotate at high speed; however, the number of high-speed commercial machine tools is very limited. This study performed cutting experiments using an air-turbine spindle of 80,000 rpm attachable to the spindle of a high-speed machining center. We examined the cutting force characteristics for the applicability of the air-turbine spindle to micro end milling.

The micro groove machining was performed by a micro end mill with a diameter of 200 μm. The workpiece is Al6061-T6. The tool edge radius was about 1.0 μm measured by SEM. Fig. 3 is the SEM picture of the micro end mill used in this experiment. The good responsiveness of a tool dynamometer is required to obtain the cutting force in high-speed milling. This study used a newly developed tool dynamometer for micro machining with a built-in force sensor. Reliable cutting force signals could be acquired with the newly developed tool dynamometer. The calibration of the tool dynamometer was installed on a Kistler 9257B and was compared to the output signals. The sensitivity was adjusted for each axis direction. The sensitivity of the force sensor was set at -7.84pC/N for the x-axis, -7.90pC/N for the y-axis and -3.78pC/N for the z-axis. For the insulation of the tool dynamometer, nickel was coated on the surface. The cutting force signal was obtained through a charge amplifier and a digital oscilloscope. A cutting origin was set through a CCD camera. Fig. 4 and Table 1 show the experimental set-up and the specification of instruments.

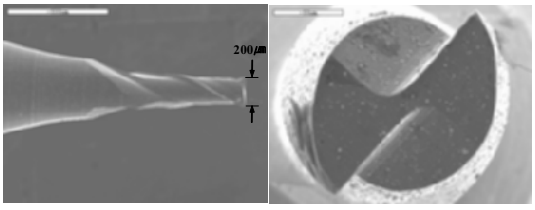

(a) Side view (b) Top view

Fig. 3. SEM pictures of micro end mill.

As for the cutting conditions, the feed per tooth was selected at 1.0-5.0 μm/tooth. The spindle revolution was fixed at 62,000 rpm, which is a stable operation speed for an air-turbine spindle. A 2-flute flat end mill was used and the size of the workpiece was 20 × 20 × 10 mm. Table 2 indicates the cutting conditions for the verification experiment of the cutting force model.

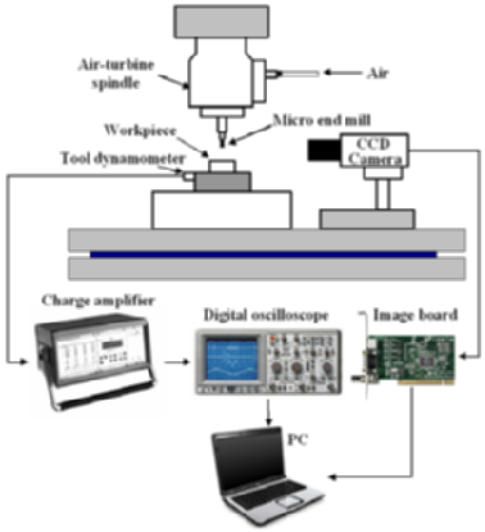

Fig. 4. Experimental setup.

Table 1. Specification of experimental instruments.

Instrument	Specification
Machining center	Makino V55
Air-turbine spindle	BIG BBT40(Max. 80,000 rpm)
Charge Amplifier	Kistler 5019 A
Digital oscilloscope	LeCroy 9330 A(200 MHz)
Tool dynamometer	Built-in with force sensor Kistler 9251 A
CCD camera	Neocom(x450)

Table 2. Cutting conditions.

Spindle revolution	62,000 rpm
Feed per tooth	1.0 ~ 5.0 μm /tooth
Radial depth of cut	200 μm
Axial depth of cut	20 μm
Tool	WC 2-flute flat endmill (TiAlN coated) Tool diameter=200 μm, $r_T \approx$ 1.0 μm, β=30°
Workpiece	Al6061-T6(K=410 MPa, Y=270 MPa, n=0.05)

4. Results and discussions

Fig. 5 shows the predicted results of the principal cutting force and thrust force according to the undeformed chip thickness. When the undeformed chip thickness is below 1.5 μm, the thrust force is larger than the principal cutting force. In Fig. 6, F_{CS} and F_{TS} are the calculated force components by the shearing, and F_{CM} and F_{TM} are the calculated force components by the ploughing and sliding, where F_{CS} and F_{CM} are the principal directions and F_{TS} and F_{TM} are the thrust directions. When the undeformed chip thickness is below 1.5 μm, F_{CM} is 31% of the total cutting force in the principal direction and F_{TM} is 54% of the total cutting force in the thrust direction. However, as the undeformed chip thickness increases above 1.5 μm, the portion of F_{CM} and F_{TM} is reduced. The ploughing and sliding could be expected to contribute to the thrust force when the tool edge radius comes to be on the order of the undeformed chip thickness. While the thrust force in the conventional end milling model was supposed to be 30% of the principal cutting force [4], in micro end milling, the thrust force becomes larger than the principal cutting force due to the ploughing and sliding. Therefore, the existing cutting force models would be limited to predicting cutting force behavior in micro end milling.

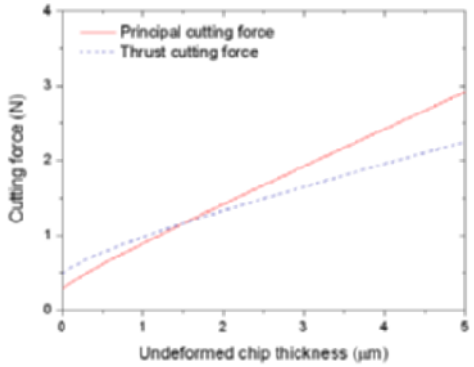

Fig. 5. Predicted principal and thrust cutting force according to undeformed chip thickness.

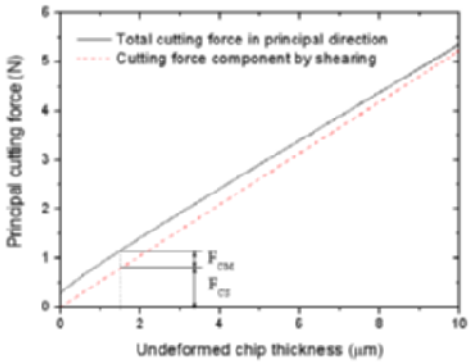

(a) Principal direction

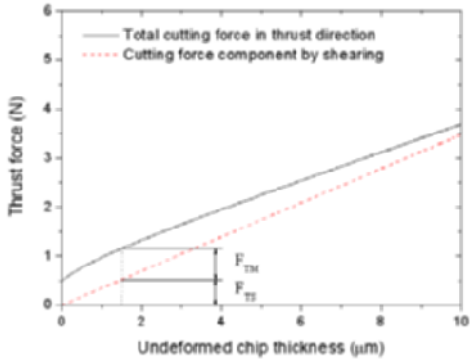

(b) Thrust direction

Fig. 6. Decomposition of cutting forces.

Figs. 7-9 show the predicted and experimental cutting forces. Except for the difference in the maximum

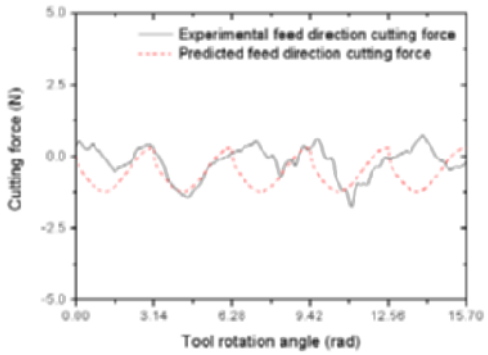

(a) Feed direction

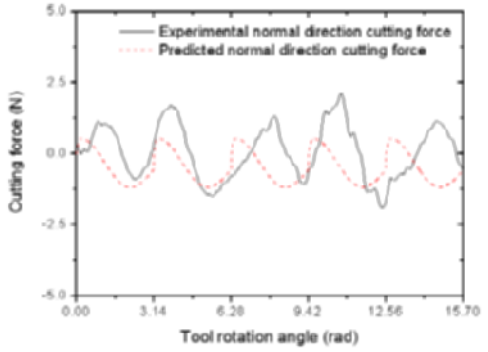

(b) Normal direction

Fig. 7. Comparison of experimental and predicted cutting force for feed per tooth of 1.0 μm.

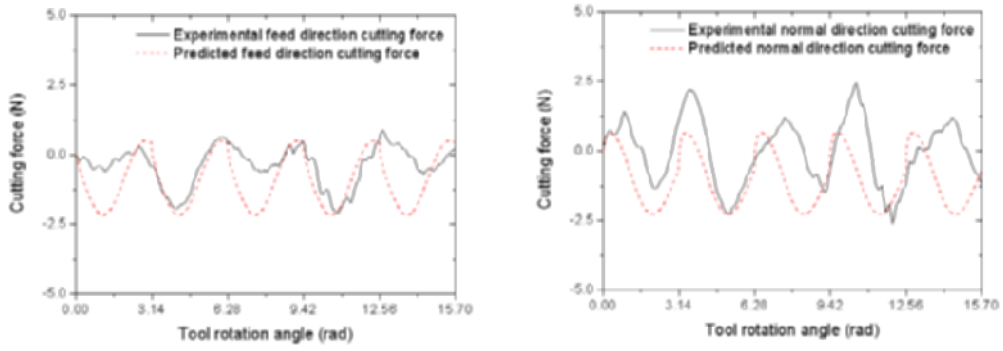

(a) Feed direction (b) Normal direction

Fig. 8. Comparison of experimental and predicted cutting force for feed per tooth of 3.0 μm.

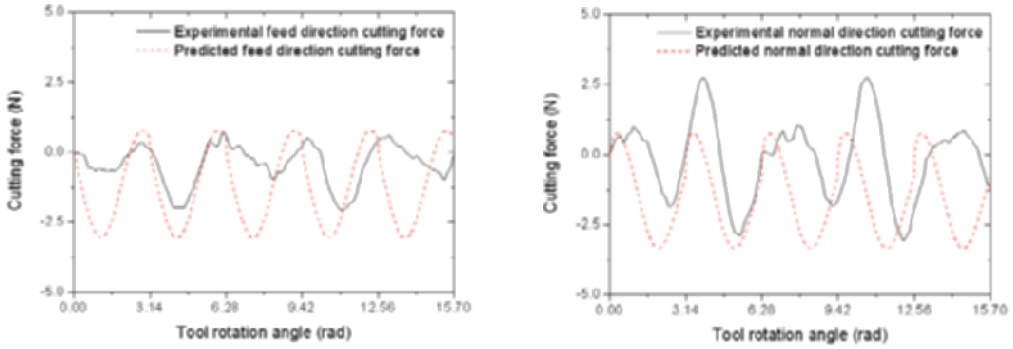

(a) Feed direction (b) Normal direction

Fig. 9. Comparison of experimental and predicted cutting force for feed per tooth of 5.0 μm.

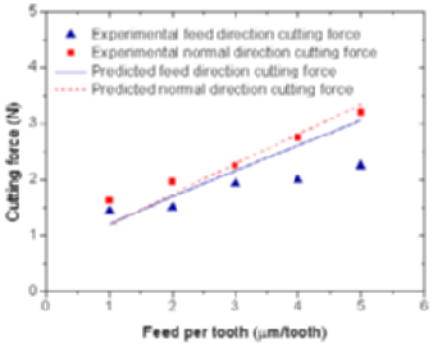

Fig. 10. Comparison of experimental and predicted maximum cutting force according to feed per tooth.

normal direction cutting force, which may be caused by tool runout [14, 15], the experimental results are similar with the predicted results. Fig. 10 shows the maximum predicted and experimental cutting forces according to feed per tooth. When the feed per tooth is 1.0 μm, the predicted cutting force shows that there is not a difference between the feed and normal direction cutting forces. This means that an increase in the thrust force due to the ploughing and sliding has a greater influence on the feed direction cutting force. This phenomenon where the thrust force becomes larger than the principal cutting force can influence the precision of micro machined parts. Such a phenomenon affects the surface integrity through residual stress and the plastic deformation of the subsurface of the material rather than chip formation in micro cutting. The results show that the normal direction cutting forces gradually become larger than the feed direction cutting forces as the feed per tooth increases above the tool edge radius. However, the increase in the cutting force can lead to a decrease in tool life and tool fracture. Accordingly, for micro end milling process, it is necessary to investigate precise cutting force predictions that take into account the character-

istics of micro cutting.

5. Conclusions

This study presented a prediction of cutting force in micro end milling in which the effect of the tool edge radius is considered. To verify the predicted results and examine the actual cutting force characteristics, we performed cutting experiments on aluminum using a micro end mill with a diameter of 200 μm.

By the proposed cutting force model, the ploughing and sliding contribute to the thrust force when the tool edge radius comes to be on the order of the undeformed chip thickness. In addition, it is found that the increasing of thrust force affects the feed direction cutting force in micro end milling with a very small feed per tooth. The characteristics of the predicted cutting forces were similar to the experimental results. This investigation for cutting force characteristics can be used for the micro tool design and process control of micro machining.

Acknowledement

This study was financially supported by Pusan National University in program. Post-Doc. 2007.

References

[1] T. Masuzawa, State of the art of micromachining, Ann. CIRP Keynote 49 (2) (2000) 473-488.

[2] L. Alting, F. Kimura, H. N. Hansen and G. Bissacco, Micro engineering, Ann. CIRP Keynote 52 (2) (2003) 635-658.

[3] M. E. Martellotti, An analysis of the milling process, Trans. ASME 63 (1941) 677-700.

[4] J. Tlusty and P. MacNeil, Dynamics of cutting forces in end milling, Ann. CIRP 24 (1) (1975) 21-25

[5] W. A. Kline and R. E. DeVor, The effect of cutter runout on cutting geometry and forces in end milling, Int. J. Mach. Tool Des. Res. 23 (1983) 123-148.

[6] G. Yucesan, A. E. Bayoumi and L. A. Kendall, An analytical cutting force model for milling, Trans. NAMRI/SME (1990) 137-145.

[7] W. Y. Bao and I. N. Tansel, Modeling micro-end-milling operations. Part I: analytical cutting force model, Int. J. Mach. Tools Manuf. 40 (15) (2000) 2155-2173.

[8] D. A. Lucca and Y. W. Seo, Effect of tool edge geometry on energy dissipation in ultraprecision machining, Ann. CIRP 42 (1) (1993) 83-86.

[9] C. Arcona and T. A. Dow, An empirical tool force model for precision machining, Trans. ASME J. Manuf. Sci. Eng. 120 (1998) 700-707.

[10] S. J. Heo, Micro cutting of tungsten carbides with SEM direct observation method, Int. J. KSME 18 (5) (2004) 770-779.

[11] I. S. Kang, J. S. Kim, J. H. Kim, M. C. Kang and Y. W. Seo, A mechanistic model of cutting force in the micro-end-milling process, J. Mater. Process Technol. 187-188 (2007) 250-255.

[12] D. A. Lucca, R. L. Rhorer and R. Komanduri, Energy dissipation in the ultraprecision machining of copper, Ann. CIRP 40 (1) (1991) 69-72.

[13] S. M. Son, H. S. Lim and J. H. Ahn, A study on the critical depth of cuts in micro grooving, Int. J. KSME 17 (2) (2003) 239-245.

[14] H. Q. Zheng, X. P. Li, Y. S. Wong and A. Y. C. Nee, Theoretical modeling and simulation of cutting forces in face milling with cutter runout, Int. J. Mach. Tools Manuf. 39 (12) (1999) 2003-2018.

[15] W. Y. Bao and I. N. Tansel, Modeling micro-end-milling operations. Part II: tool run-out, Int. J. Mach. Tools Manuf. 40 (15) (2000) 2175-2192.